

Using stop bar detector information to determine turning movement proportions in shared lanes

Ali Gholami* and Zong Tian

Department of Civil & Environmental Engineering, University of Nevada, Reno, Reno, NV 89557, USA

SUMMARY

Turning vehicle volumes at signalized intersections are critical inputs for various transportation studies such as level of service, signal timing, and traffic safety analysis. There are various types of detectors installed at signalized intersections for control and operation. These detectors have the potential of producing volume estimates. However, it is quite a challenge to use such detectors for conducting turning movement counts in shared lanes. The purpose of this paper was to provide three methods to estimate turning movement proportions in shared lanes. These methods are characterized as flow characteristics (FC), volume and queue (VQ) length, and network equilibrium (NE). FC and VQ methods are based on the geometry of an intersection and behavior of drivers. The NE method does not depend on these factors and is purely based on detector counts from the study intersection and the downstream intersection. These methods were tested using regression and genetic programming (GP). It was found that the hourly average error ranged between 4 and 27% using linear regression and 1 to 15% using GP. A general conclusion was that the proposed methods have the potential of being applied to locations where appropriate detectors are installed for obtaining the required data. Copyright © 2016 John Wiley & Sons, Ltd.

KEY WORDS: intersection detector; shared lane; turning vehicle volume; regression; genetic programming

1. INTRODUCTION

Turning vehicle volumes at intersections are not only needed for intersection operational analyses, e.g., level of service (LOS) and signal timing, but also serve as key inputs for traffic safety studies and travel demand modeling. In traffic operational studies, turning volumes are needed for intersection and arterial LOS analysis. In traffic safety studies, intersection and link volumes are needed to calculate crash rates, develop safety performance functions, and rank high crash locations. In transportation planning, intersection and link volumes are major inputs for calibrating travel demand models. While many Departments of Transportation (DOTs) have installed a large number of volume counting stations along major freeway and arterial routes, the majority of urban arterial streets are not covered. One of our previous studies indicated that less than 5% of the roadway segments were covered by the Nevada Department of Transportation's permanent counting stations in order to fulfill the SafetyAnalyst requirements. Additionally, these counting stations only provide directional volume counts that are not sufficient for operational analysis. Currently, intersection volumes are primarily obtained through manual counting, which is labor-intensive and unsafe. This paper proposes new methods to automatically collect turning volumes in shared lanes using existing signal control and detection devices. These devices are already in place at most signalized intersections, and they have the capabilities of archiving high-resolution signal timing and detector information. These methods only use stop bar detectors to provide automated turning volume counts in shared lanes. Traffic volumes can be continuously collected at a low cost, which fulfills the needs for various transportation studies. Various divisions at state DOTs, such as Traffic Operations, Safety Engineering,

*Correspondence to: Ali Gholami, Department of Civil and Environmental Engineering, University of Nevada, Reno, Reno, NV 89557, USA. E-mail: agholami@unr.edu

Transportation and Intermodal Planning, Traffic Information, and Performance Analysis, would benefit from this study.

2. BACKGROUND SUMMARY

Technologies on automated traffic volume counts at roadway segments are relatively mature. An increasing number of large urban freeways in the USA have implemented flow detectors to automatically gather volume, speed, and occupancy data. Various detection technologies exist, including inductive loops, pneumatic tubes, magnetic sensors, video, radar, and microwave detectors. However, these technologies have not been widely used for obtaining turning movement volumes at intersections. The difficulties in automated turning movement counts lie in the fact that multiple detectors need to be placed in order to track the turning traffic. In current practice, turning movement volumes are mostly obtained through manual counts that prove to be costly and dangerous to the conducting personnel. Therefore, research on automatic turning movement counts at intersections has drawn major interest over the past decade.

A number of research efforts attempted to use videos (either video detection systems or videotaping) coupled with data extraction software, to estimate turning movement volumes at intersections. Tian *et al.*[1] developed a system called time and place system, which extracts turning movement data from several video detectors. Miovision Technologies Inc. developed a portable intersection video recording system that extracts the turning volumes from videos using their in-house software. Such technologies still require installation of video equipment each time a count is desired. The cost can be high if a large number of sites are covered. Furthermore, video-based technologies heavily rely on the camera view, which could be restricted by the physical layout of an intersection. Other nonvideo-based tools aim to provide real-time estimates for turning movement proportions [2–4]. Such efforts focused on improving adaptive signal control systems. Various algorithms were developed based on limited detector information to derive turning movement proportions, from which turning volumes can be derived by the total link volumes.

Obtaining turning volume counts from detectors in shared lanes is a major challenge; thus, multiple detectors are often needed to track the turns [5, 6]. Loops must be located at strategic locations at the stop bar and downstream of the intersection. Furthermore, based on the network traffic flow patterns, some intersections' turning estimates can provide approximations for adjoining intersections [7], or conversely, the path flow can provide approximations for estimation of turning movements [8].

Some cities, including Seattle, San Antonio, and Toronto, provide real-time or stored travel information on selected freeways and arterials. The information is received at their traffic management centers from a network of inductive loop detectors.

Metropolitan Toronto reported the development of a prototype transit and traffic information system [9]. The goal was to incorporate freeway and arterial SCOOT (Split, Cycle and Offset Optimization Technique) data into a complete user information data system. The system is called COMPASS and is employed on some sections of the Queen Elizabeth Way as well as Highway 401. In this system, data is collected at 20-s intervals and aggregated to 5-min, 15-min, 1-h daily and monthly time periods. Volume, occupancy, and speed data are archived for the 20-s and 5-min time intervals. The San Antonio TransGuide program has been warehousing traffic information from over 300 detector stations located on freeway mainline segments and ramps. Speed, volume, and occupancy data are all stored in their database [9]. ITE reports that four cities, Nashua, NH; Fremont, CA; Minneapolis/St. Paul, MN; and Bellevue, WA, are collecting traffic counts using their loop detector systems [10].

Today, most vehicle detection relies on inductive loop detectors. However, problems with installation and maintenance of these detectors have necessitated evaluation of alternative detection systems. Replacing loops with better detectors requires a thorough evaluation of the alternatives. Alternative detection technologies include video image detection, radar, Doppler microwave, and passive acoustic. Several studies have compared these technologies with loop detectors, and results clearly indicate promising nonintrusive alternatives to loops, but their limitations must be understood [11, 12].

Vanajakshi and Rilett [13] and Bender and Nihan [14] reviewed studies regarding the accuracy of loop detector counts and improvement algorithms. Jacobson *et al.* divided loop detector data screening

tests into two main categories: microscopic and macroscopic [15]. At the microscopic level, detector pulses are scanned and checked for error in the field. At the macroscopic level, volumes from detectors are collected from the sites and are compared with manual counts. Some researchers, such as Dudek *et al.* [16], Courage *et al.* [17], Pinnell [18], Bikowitz and Ross [19], and Chen and May [20] have addressed the causes and effects of loop detector data errors. Studies of loop detector data errors at the microscopic level usually require reprogramming or modification of the detector device and depend on the loop detector type [10, 21, 22]. However, macroscopic approaches are more commonly adopted because they are independent of the sensor type and are carried out at the data processing level [22]. Common macroscopic studies compare volumes, occupancies, or speeds with specific threshold values [21, 23, 24].

A review of prior studies and current technologies indicate that there is no automated method to calculate the proportion of turning movement volumes in shared lanes without downstream detectors (also known as departure or exit detectors). Most studies rely on additional downstream detectors to estimate the shared lane turning volume [1–6], while many intersections do not have such detectors. Modern signal controllers are enhanced with advanced data monitoring and logging capabilities, making it possible to record high-resolution detector and signal timing information. The methods proposed in this paper can be used to estimate turning movement volumes in shared lanes using such information. This provides continuous traffic volume counts without incurring additional costs.

3. METHODOLOGY

Three methods proposed in this paper to estimate shared lane turning volume proportions based on stop bar detectors include: (1) network equilibrium (NE) that utilizes the actual upstream and downstream counts at other intersections, (2) volume and queue (VQ) of shared lanes compared with adjoining lanes, and (3) flow characteristics (FC) of shared lanes. These methods do not work together and need to be applied separately. Because each method has its limitations and cannot be used for all shared lanes, these methods are proposed as alternative options and when one works for one condition, it is not necessary to use the other ones. Obtaining turning volumes manually in the field remains a necessary method at intersections where there is no possibility of using these methods.

3.1. Network equilibrium

The NE method has been mentioned by Gentili and Mirchandani [7]; however, it is explained in this paper to complete the list of possible methods. Based on volume equilibrium, it is possible to estimate shared lane proportion if there are enough equations for every unknown movement. For example, Figure 1 displays a simple network where there are two intersections. The following equation can be applied to calculate westbound through at intersection i :

$$WT_i^t = -NL_i^t - SR_i^t + WR_j^{t+\Delta t} + WT_j^{t+\Delta t} + WL_j^{t+\Delta t} - \delta_{ij}^t \quad (1)$$

where

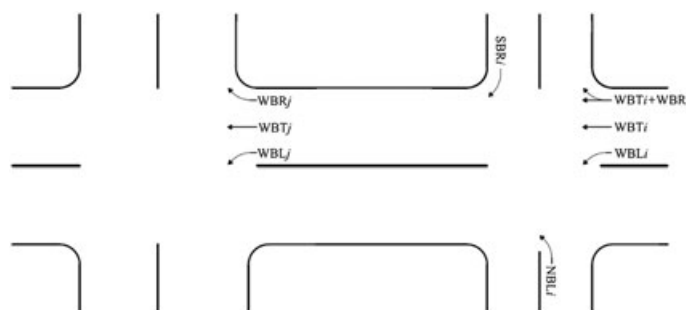


Figure 1. Example network with two intersections.

- WT* westbound through
- NL* northbound left
- SR* southbound right
- WR* westbound right
- WL* westbound left
- t* time interval *t*, for example, 7:00:00 to 7:15:00
- i,j* intersection numbers
- Δt travel time between intersections *i* and *j*
- $\delta_{ij}^{t+\Delta t}$ additional trips generated between intersections *i* and *j* during time interval *t*

If the distance between two intersections is short or there are no significant volume fluctuations during different time intervals, Δt can be assumed as zero. Also, $\delta_{ij}^{t+\Delta t}$ can be considered zero if there is no major trip generator between intersections *i* and *j*. The advantage of this method is that high-resolution detector data and traffic signal information are not required. A low-cost approach to obtaining detector and signal timing information is through advanced signal control software. Technologies in signal control systems have advanced dramatically in recent years. The latest signal control hardware and software are equipped with enhanced features for providing high-resolution detector and signal timing information. Figure 2(a) displays automatically reported detector information from an existing intersection in Reno, Nevada. This data sample shows the vehicle counts from the detectors aggregated in 15-min intervals.

Volume Report



		Detectors							
Date/Time		9'	10'	11'	12'	5'	6'	7'	8
46 KIETZKE & MOANA									
6/12/2013	6:00:00AM	29	33	45	41	0	0	0	0
6/12/2013	6:15:00AM	26	36	39	37	0	0	0	0
6/12/2013	6:30:00AM	33	32	57	53	0	0	0	0
6/12/2013	6:45:00AM	46	67	89	87	0	0	0	0
.
.

a) 15-minute aggregated data

- 08:09:15.012, D8 on, 7.902s → Detector #8 on at 08:09:15.012; Vacant time is 7.902s
- 08:09:15.481, D8 off, 0.468s
- 08:09:16.761, G3 off, 29.389s → Green Phase #3 off at 08:09:16.761; Green duration time is 29.389s
- 08:09:16.761, Y3 on, 179.021s
- 08:09:17.620, D9 on, 2.686s
- 08:09:18.151, D10 on, 2.593s
- 08:09:18.307, D9 off, 0.687s → Detector #9 off at 08:09:18.307; Occupy time is 0.687s
- 08:09:18.823, D10 off, 0.671s
- 08:09:20.244, Y3 off, 3.482s → Yellow Phase #3 off at 08:09:20.244; Yellow duration time is 3.482s
- 08:09:21.649, D22 on, 80.953s
- 08:09:22.008, D22 off, 0.359s
- 08:09:23.242, G1 on, 172.806s → Green Phase #1 on at 08:09:23.242; Red duration time is 172.806s

b) High resolution data

Figure 2. Sample of aggregated and high-resolution data.

3.2. Volume and queue length of shared lanes

There are some cases where a shared lane has some adjoining lanes with similar movements. For this condition, the probability that a vehicle stays in the shared lane while its queue length is longer than the adjoining lane(s) would be very low. This probability depends on driver habits, the upstream and downstream intersection configuration, and distance to the intersection. Figure 3 demonstrates the intersection at Eighth Street and Center Street in Reno, Nevada. At the westbound approach, there are two exclusive lanes and one shared lane. Field observations show that when there are several vehicles in the shared lane while the other two through lanes are less congested, it is likely that most vehicles in the shared lane would turn right. There might be an association between the ratio of shared lane volume to the adjoining lane volumes and the ratio of right turns to through volumes in shared lanes. The following equations demonstrate this association:

$$r_{s,a}^t = \frac{v_s^t}{v_a^t} \quad (2)$$

$$r_{r,t}^t \text{ (or } r_{l,t}^t) = \frac{v_r^t \text{ (or } v_l^t)}{v_t^t} \quad (3)$$

$$r_{r,t}^t \text{ (or } r_{l,t}^t) = f(r_{s,a}^t) \quad (4)$$

where

$r_{s,a}^t$	ratio of shared lane volume to volume of adjoining lanes with same direction at time interval t
$r_{r,t}^t \text{ (or } r_{l,t}^t)$	ratio of right (or left) turns to through volume in shared lane at time interval t
v_s^t	total volume in shared lane at time interval t
v_a^t	total volume at adjoining lane(s) at time interval t , for example, if shared lane is right and through, then all adjoining through lanes should be considered
$v_r^t \text{ (or } v_l^t)$	total right (or left) turns in shared lane at time interval t
v_t^t	total through volume in shared lane at time interval t

After developing Equation 4 for each shared lane, the turning volumes may be estimated. Note that this method is applicable only for shared lanes that have at least one adjoining lane with similar movement. In addition, some shared lanes are wide enough for right-turn vehicles to overpass stopped vehicles to make their turns. At these shared lanes, this method cannot be used.

The advantage of this method is that high-resolution detector data and signal timing information are not required. However, shorter time intervals (for instance, 1 min) would yield better results.

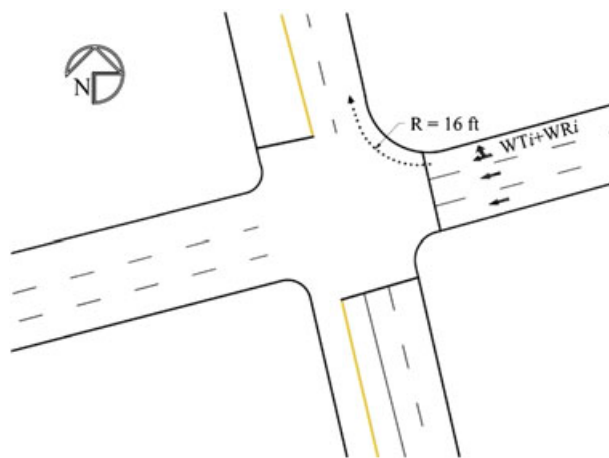


Figure 3. Intersection of Eighth Street and Center Street, Reno, NV.

Usually, this method can be used if the downstream intersection is not so close to the study intersection because some vehicles use more congested lanes because of their turning movement at the next intersection.

3.3. Flow characteristics of shared lanes

If there is high-resolution data from stop bar detectors and traffic signal data, then it would be possible to develop an estimation model based on vehicle headways in shared lanes. The turning movement can be related to headway, the position of a vehicle in the queue, and vehicle type. Also, intersection geometry can affect the significance of headway on the turning movements. Here, the geometry can be be summarized as the turning radius. The turning radius depends on whether the shared lane is a right or left turn, the number of lanes accessible for turning vehicles, width of each lane, angle of turning, and number of opposing lanes. Figure 4 demonstrates the problem. The probability of vehicle *i* turning right (or left) could be related to time headway, and time headway is a function of vehicle type, headway of front vehicle, type of front vehicle, and position of vehicle in the line. Therefore, the probability of vehicle *i* turning right (or left) could be a function of all of these parameters as it is shown in Equation (5).

$$P(t_{i,r}) \text{ or } P(t_{i,l}) = f(h_i, hf_i, cp_i, ct_i, cf_i) \tag{5}$$

where

- $P(t_{i,r}) \text{ or } P(t_{i,l})$ probability of vehicle *i* turning right (or left)
- h_i headway, the time difference of vehicle *i* from its front vehicle when passing stop bar
- hf_i summation of each headway with previous car headway
- cp_i position of vehicle *i* in the line
- ct_i type of vehicle *i*
- cf_i type of front vehicle of vehicle *i*

In this method, when the turning radius is large, the difference between the headways of through and turning vehicles is not significant. Therefore, the first step is to check the applicability of this method for an intersection based on turning radius. In other words, to use this method, there must be an association between turning movement and headway.

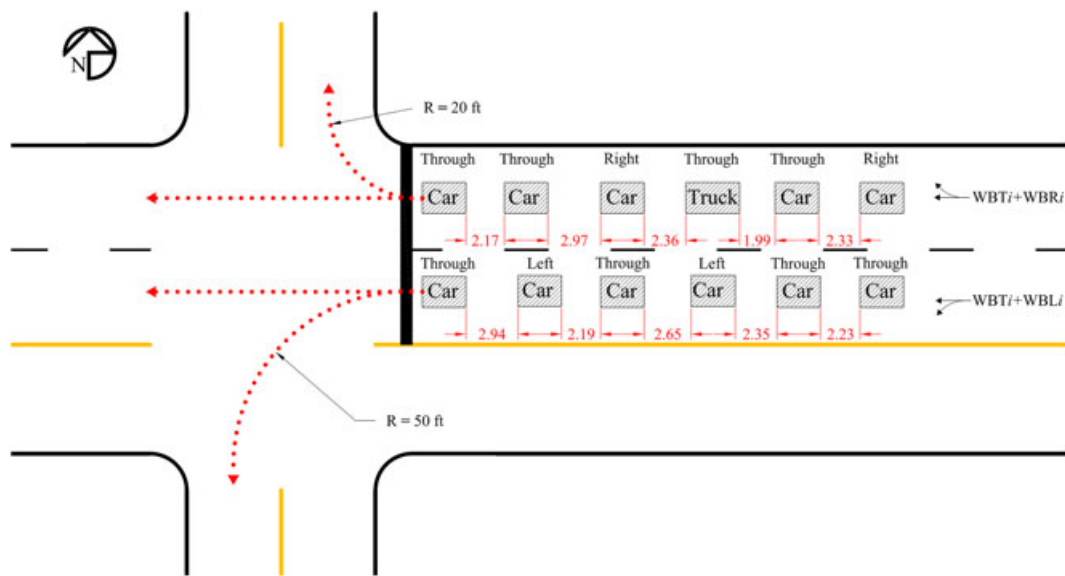


Figure 4. Headway in shared lanes.

One critical step of any volume counting system is to attain signal timing and detector information. Most of the previous studies relied on additional data recording devices in order to obtain detailed data. The Texas Transportation Institute (TTI) developed a data acquisition toolbox that can be directly connected to a TS2 controller cabinet [25]. The TTI toolbox has a hardware and software tool to automatically download detector information and summarize various performance measures. This toolbox can record high-resolution detector and signal timing data and work with any NEMA (National Electrical Manufacturer's Association) signal control cabinet. Sample data was collected using the device as shown in Figure 2(b). As can be seen, the on/off times of each detector and signal phase are recorded at the millisecond resolution.

An issue regarding this method is the vehicles that arrive during green time when there is not a queue. These vehicles are not lined up during the red time. As a result, their headway is random and generates noise in the model. One method to deal with this issue is to share these vehicles with ratio of vehicles that have headway significantly related to turning vehicles. Furthermore, the first vehicle in the queue should be divided between through and right (or left) turn based on this ratio.

If the shared lane is a through and right turn and the intersection is not a no turn on red (NTOR), all vehicles that activate the detector during red time are categorized as a right turn. At such intersections, if pedestrian volume at the cross street is high, the through and turning headways lose their significance. Similar to the VQ method, some shared lanes are wide enough for right-turn vehicles to overpass stopped vehicles in order to make their turns. At these shared lanes, this method cannot be utilized.

One of the factors that make headway a significant parameter on turning vehicles is drivers' behavior. In some cities, drivers are more conservative and keep a slower speed during turning. In other cities, the difference between speed of turning and through vehicles is not significant. In addition, observations show that driver behavior changes during peak hours. However, the effects of these factors can be summarized as the significant difference of through vehicles compared with turning vehicles and should be tested by a pilot study.

Table I summarizes the advantages, disadvantages, and applicable conditions of these three methods.

Table I. Advantages, disadvantages, and applicable conditions of proposed methods.

Modeling method	Advantages (+) and disadvantages (-)	Considerations
Flow characteristics	<ul style="list-style-type: none"> + Applicable for most of intersections - It depends on drivers' behaviors 	<ul style="list-style-type: none"> •The turning radius should not be too large •There should not be too much pedestrian crossing the street during turning green time •When using for left turn, left turn must be protected •If there is more than one activation in through and right-turn shared lane during red time, then these extra activations should be considered right turn. Even for no turn on red intersections, this can be applied because drivers frequently violate no turn on red for right turn.
Volume and queue	<ul style="list-style-type: none"> + Both 1-min aggregated and high-resolution data can be used - It depends on drivers' behaviors - It does not produce good results if the study intersection is too congested 	<ul style="list-style-type: none"> •There should not be another intersection in downstream close to the study intersection
Network equilibrium	<ul style="list-style-type: none"> + Both aggregated and high-resolution data can be used + It does not depend on drivers' behaviors - It needs data from another (downstream) intersection 	<ul style="list-style-type: none"> •There should not be a significant trip generator between two intersections •It is possible to use advance detectors of downstream intersection instead of its stop bar detectors.

3.4. Observed proportions in the field

When none of these three methods can be applied, observed proportions in the field can be applied for future estimates. This means that the proportion of turning volumes at each time interval would be applied in the future as long as there is an insignificant difference between turning proportions during different days, weeks, and months.

4. CASE STUDY

The methods provided in this paper were applied at three different intersections in Reno, Nevada. In the following sections, the case of each method is described.

4.1. Network equilibrium

The intersection at Ninth Street and Sierra Street, shown in Figure 5, was selected for the NE method. At this intersection, eastbound through and eastbound right share a lane. All required movements for calculating the proportion of this shared lane have a loop detector. The two unknown movements can be calculated using the following equations:

$$ER_i^t = -SR_j^t - ST_j^t + ST_i^t + WL_i^t \tag{6}$$

$$ET_i^t = -ET_k^t - EL_k^t - ER_k^t + SL_i^t + NR_i^t \tag{7}$$

where

- ER eastbound right
- SR southbound right
- ST southbound through

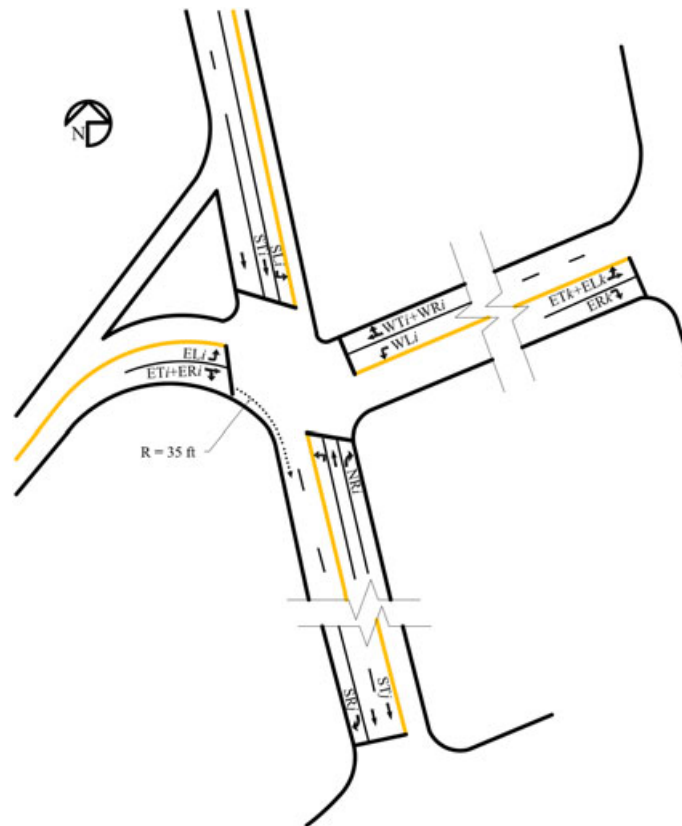


Figure 5. Intersection of Ninth Street and Sierra Street, Reno, NV.

<i>WL</i>	westbound left
<i>ET</i>	eastbound through
<i>EL</i>	eastbound left
<i>SL</i>	southbound left
<i>NR</i>	northbound right
<i>t</i>	time interval <i>t</i> , for example, 7:00:00 to 7:15:00
<i>i, j, k</i>	intersection numbers

The travel time between intersections *i* and *j* or *k* is very short. As a result, Δt has been considered zero. In addition, there is not a significant trip generation between intersections *i* and *j* or *k*. Therefore, additional trips generated between intersections *i* and *j* or *k* during time interval *t*, $\delta_{ij}^{t+\Delta t}$ or $\delta_{ik}^{t+\Delta t}$, have been ignored.

4.2. Volume and queue length of shared lanes

The intersection at Eighth Street and Center Street displayed in Figure 3 was selected for the VQ method because at this intersection, adjacent lanes of the shared lane have similar movements. For the westbound approach, there are two exclusive lanes and one shared lane for right and through movements. A prediction model was established for this shared lane. Table II shows the sample of data gathered for this intersection. Two sets of data similar to this table were made: one for model development and another one for model validation.

4.3. Flow characteristics of shared lanes

To test the validity of the FC method, several shared lanes with different turning radii were required because turning radius is one of the factors that affect the significance of headways. These intersections are westbound shared lane at the intersection of Eighth Street and Center Street in Figure 3, with a turning radius equal to 16 ft; the eastbound shared lane at the intersection of Ninth Street and Sierra Street in Figure 5, with a turning radius equal to 35 ft; and the northbound shared lane at the intersection of North McCarran Blvd and Clear Acre Ln in Figure 6, with a turning radius equal to 100 ft.

For each of the shared lanes, collected data was tabulated, and the sample can be seen in Table III. Two sets of data similar to this table were made: one for model development and another one for model validation. In these tables, headway, h_i , is the time difference between the vehicle *i* and the front vehicle when passing the stop bar. The next column, hf_i , is the summation of each headway with the previous vehicle's headway. The reason for defining this variable is that the front car headway can affect the headway of the following car. Car position, cp_i , means the position of the car in the line. Car type, ct_i , was also added as a variable because it is likely that heavy vehicles have lower speeds, thus resulting in a higher headway. Because of propagation of this effect to following cars, front car type variable, cf_i , was also added. Lastly, td_i , shows the turning direction of cars. This variable was used as the response variable, while others remain independent variables.

Table II. Sample of data collected for volume and queue method at intersection of Eighth Street and Center Street, Reno, NV.

Time interval (1 min)	Shared lane volume	Adjoining lane(s) volume	Ratio of shared lane to adjoining lanes	No. of right turns	Ratio of right turns
<i>t</i>	v_s^t	v_a^t	$r_{s,a}^t$	v_r^t	$r_{r,t}^t$
1	6	25	0.24	3	0.50
2	7	18	0.39	5	0.71
3	6	13	0.46	4	0.67
4	18	21	0.86	18	1.00
5	7	16	0.44	5	0.71

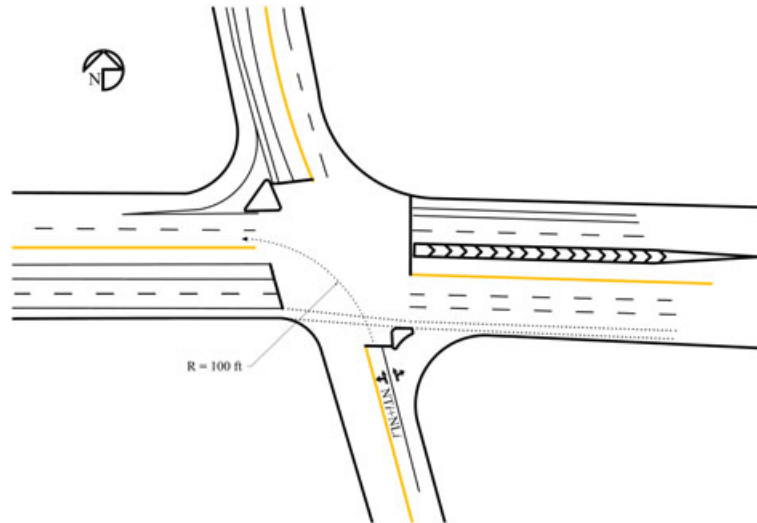


Figure 6. Intersection of North McCarran Blvd and Clear Acre Ln, Reno, NV.

Table III. Sample of data collected for flow characteristics method at intersection of Eighth Street and Center Street, Reno, NV.

Cycle no. cn_j	Headway h_i	Front car headway hf_i	Car position cp_i	Car type ct_i	Front car type cf_i	Turning direction td_i
1	0	0	1	c	c	T
1	2.24	2.24	2	c	c	R
1	2.31	4.55	3	t	c	T
1	3.01	5.32	4	c	t	T

c, private car; t, truck; T, through; R, right turn.

5. DATA ANALYSIS

5.1. Modeling

The NE method needs direct calculation and does not require prediction models. For the VQ method, linear regressions and for FC method generalized linear model were performed in R®. VQ was modeled as a continuous variable and FC as discrete. R® was able to generate models for both continuous and discrete variables. Genetic programming (GP) was also used for modeling. GP is an evolutionary algorithm-based methodology that can develop a model based on a set of data. GP was generally able to find a more accurate model compared with other conventional methods.

GP was greatly stimulated in the 1990s by John Koza. GP applies the same evolutionary approach as genetic algorithms. However, GP is no longer breeding bit strings that represent coded solutions but is a complete computer program that solves a problem at hand. In making a model using conventional methods like regression, the user needs to define the structure of the model. For nonlinear and complex data, this task is challenging especially when there is more than one variable. The user does not need to know the structure of data and evolutionary process as GP does this task.

Solving a problem by GP involves determining the set of variables, selecting the set of functions, defining a fitness function to evaluate the performance of created computer programs, and choosing the method for designating a result of the run.

Before applying GP to a problem, five preparatory steps must be accomplished [22]:

Step 1: Determining the set of terminals: The terminals correspond to the inputs of the computer program to be discovered. Our program takes three inputs: time (×1), detector volume (×2), and occupancy (×3).

- Step 2: Selecting the set of primitive functions: The functions can be presented by standard arithmetic operations, standard programming operations, standard mathematical functions, logical functions, or domain-specific functions. Our program will use four standard arithmetic operations: plus, minus, multiplication, and division, and mathematical functions square, root square, and logarithm. Terminals and primitive functions together constitute the building blocks from which GP constructs a computer program to solve the problem.
- Step 3: Defining the fitness function: A fitness function evaluates how well a particular computer program can solve the problem. For our problem, the fitness of the computer program is measured by the mean absolute percentage error (MAPE) of the results produced by the program and the observed counts. The closer MAPE is to zero, the better the computer program.
- Step 4: Deciding on the parameters for controlling the run: For controlling a run, GP uses the same primary parameters as those used for genetic algorithm. They include the population size, the maximum number of generations to be run, crossover and mutation probability, and elitism rate.
- Step 5: Choosing the method for designating a result of the run: It is a common practice in GP to designate the best-so-far generated program as the result of a run.

Once these five steps are complete, a run can be made. The run of GP starts with a random generation of an initial population of computer programs. Each program is composed of functions +, −, ×, and ÷; square, root square, and logarithm; and terminals ×1, ×2, and ×3.

In the initial population, all computer programs usually have poor fitness, but some individuals are more fit than others [26]. Just as a fitter chromosome is more likely to be selected for reproduction, a fitter computer program is more likely to survive by copying itself into the next generation. In GP, the crossover operator functions on two computer programs that are selected on the basis of their fitness. These programs can have different sizes and shapes. The two offspring programs are composed by recombining randomly chosen parts of their parents. For example, Figure 7 shows two solutions where crossover makes two offspring. For mutation, a function or terminal will be changed randomly.

After completing five preparatory steps, the following eight steps will be executed:

- Step 1: Assigning the maximum number of generations to be run and probabilities for cloning, crossover, and mutation. The sum of the probability of cloning, the probability of crossover, and the probability of mutation must be equal to one.
- Step 2: Generating an initial population of computer programs of size N by combining randomly selected functions and terminals.
- Step 3: Executing each computer program in the population and calculating its fitness with MAPE and designating the best-so-far individual as the result of the run.
- Step 4: With the assigned probabilities, a genetic operator will be selected to perform cloning, crossover, or mutation.
- Step 5: If the cloning operator is chosen, one computer program is selected from the current population of programs and will be copied into a new population. If the crossover operator is chosen, a pair of computer programs is selected from the current population and creates a pair of offspring programs. If the mutation operator is chosen, one computer program from the current population is selected to mutate, and it will be placed into the new population. All programs are selected with a probability based on their fitness (i.e., the higher the fitness, the more likely the program is to be selected).
- Step 6: Step 4 will be repeated until the size of the new population of computer programs becomes equal to the size of the initial population, N .
- Step 7: The current (parent) population is replaced with the new (offspring) population.
- Step 8: Program goes to step 3 and repeat the process until the termination criterion is satisfied.

In this paper, GPTIPS was used for generating the models. GPTIPS is a GP tool for use with MATLAB™. This package enables users to identify hidden and nonlinear relationships in data sets and automatically creates compact and accurate nonlinear equations to predict the behavior of physical systems [27, 28]. Table IV summarizes the models developed with regression, generalized linear

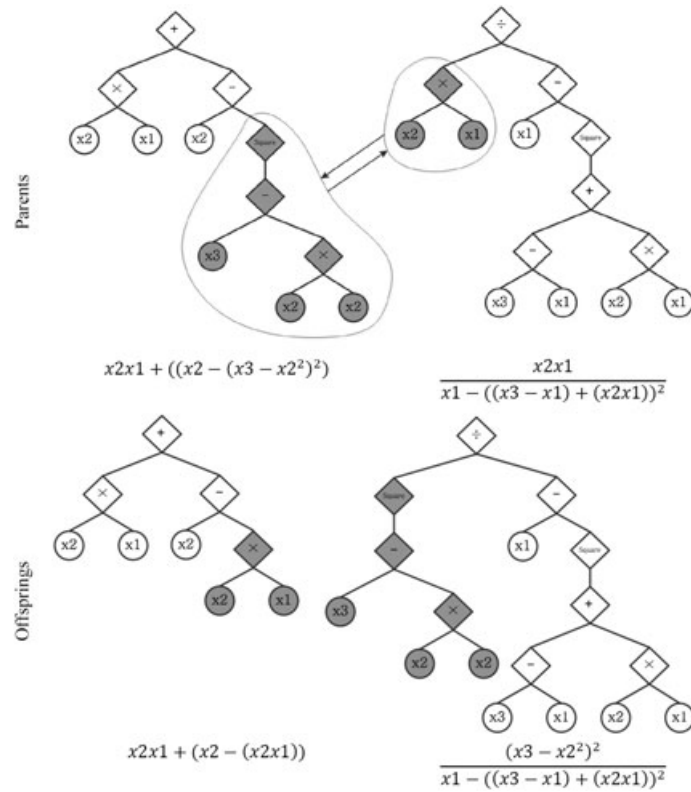


Figure 7. Crossover in genetic programming.

model, and GP for the shared lanes of this case study. Models provided with these methods are useful for short-term predictions, and as it is probable that behavior of drivers and traffic patterns change over time, models lose their validity gradually and therefore do not have long-term temporal transferability. Also, it is notable that each model is made based on the characteristics of a certain intersection. These characteristics, including traffic patterns at that intersection, traffic signal schemes, and geometry of intersection, affect the behavior of drivers, and therefore, these models cannot be used for other intersections. Also, detector configuration and accuracy affect the results. The effect of these factors would be reflected on the models. In another words, each shared lane at each intersection needs a unique model to determine its turning movement proportions.

5.2. Analysis of results

The accuracy of models was interpreted in terms of MAPE (%) and root mean squared error (RMSE) using the following equations:

$$MAPE(\%) = \frac{\sum_{i=1}^n \left| \frac{M_i - B_i}{B_i} \right|}{n} \tag{8}$$

$$RMSE = \sqrt{\frac{\sum_{i=1}^n (M_i - B_i)^2}{n}} \tag{9}$$

where

- RMSE root mean squared error (veh/15 min)
- MAPE mean absolute percentage error (%)
- M_i model estimation at lane i

Table IV. Case study lane models.

Modeling method	N Mccarran Blvd/Clear Acre Ln	Ninth St./Sierra St.	Eighth St./Center St.
Network equilibrium Regression	Not applicable	Not applicable	Not applicable
GP	Not applicable	Not applicable	Not applicable
Analytical calculation	Not applicable because of un-controlled southbound right turn	$ER_i^t = -SR_i^t - ST_i^t + WL_i^t$ $ET_i^t = -ET_k^t - EL_k^t - ER_k^t + SL_i^t + NR_i^t$	Not applicable because of downstream un-signalized intersection (Ninth St./Center St.)
Volume and queue Regression	Not applicable because the adjoining lane is also shared lane	Not applicable because of no existing same-direction adjoining lane	$r_{r,t}^t = 0.2 + 0.6 r_{s,a}^t$
GP	Not applicable because of no existing same-direction adjoining lane	Not applicable because of no existing same-direction adjoining lane	$r_{r,t}^t = 4.55 + 2.5 r_{s,a}^t - 3.75 e^{-r_{s,a}^t} + 0.25 r_{s,a}^t 2$
Analytical calculation	Not applicable	Not applicable	Not applicable
Flow characteristics Regression	$P(t_l) = \frac{e^{12.6-3.6h_l}}{1+e^{12.6-3.6h_l}} *$	$P(t_r) = \frac{e^{9.2-2.7h_l}}{1+e^{9.2-2.7h_l}} *$	$P(t_r) = \frac{e^{6-1.8h_l}}{1+e^{6-1.8h_l}} *$
GP	$P(t_l) = -3 + 2.8 \sqrt{ h_l - 3.8 } + 0.1 e^{h_l} - 0.1 h_l^2$	$P(t_r) = 1.5 + \frac{1.2 \sqrt{h_l}}{h_l-5.6} *$	$P(t_r) = 0.8 + 0.2 h_l - 0.03 e^{h_l} *$
Analytical calculation	Not applicable	Not applicable	Not applicable

GP, genetic programming.

*Other variables were insignificant (p values were bigger than 0.05) and therefore have been omitted.

B_i observed (base) count at lane i
 n total number of intervals

Figure 8 summarizes the MAPE and RMSE calculations of different methods for the case study intersections. MAPE was calculated for vehicle by vehicle and hourly average, except for the NE method, where vehicle by vehicle MAPE calculation cannot be applied. The hourly average MAPEs for all methods with GP modeling are less than 7% except at the McCarran Blvd/Clear Acre Ln intersection because of a large turning radius (100 ft). At this intersection, models showed low significance for through and turning headways, and as a result, errors were higher than the two other intersections. In the FC method, when the turning radius began to increase, the reliability of models decreased. However, a higher turning radius usually means that shared lanes have intersected with a major street. In these cases, downstream intersections of shared lanes are usually signalized. Therefore, it is feasible to use the highly accurate NE method.

In all cases, GP models were more accurate than regression, except for the hourly average of the FC method at the intersection of Ninth St. and Sierra St. where the calculated MAPE for the GP model was 2% higher than the regression method. In other cases, GP MAPE is up to 7% less. Hourly average MAPE showed that methods produced accurate turning volumes except when the turning radius was large in the FC method. In all methods, the accuracy of hourly average was greater than 85% at the case study intersections using the GP.

The RMSE were also calculated for 15-min volumes. RMSE in the FC method ranged from 8 to 70 vehicles per 15-min intervals using regression and from 12 to 37 using GP method. In the VQ method, both regression and GP have RMSE equal to 3.5 vehicles per 15-min interval. Finally in the NE method, RMSE is equal to 15 vehicles per 15 min. Note that the RMSE is sensitive to the relative volume of traffic being observed. While in reality, under and over counting of models can reduce

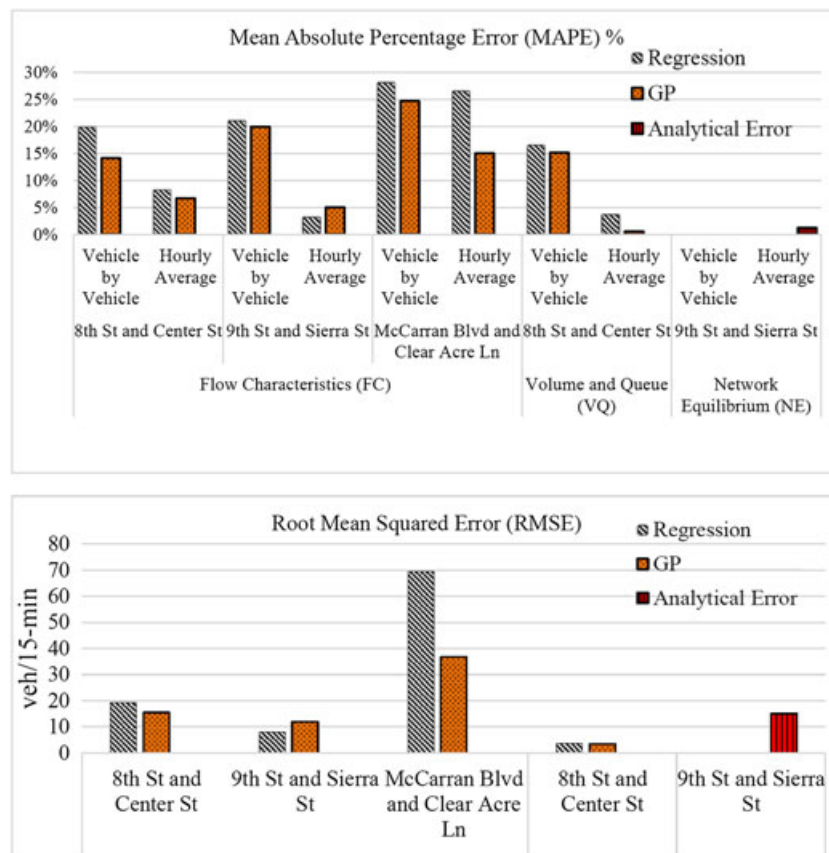


Figure 8. Mean absolute percentage error and root mean squared error of different methods at case study intersections.

the overall error, RMSE sums all the under and over counts of models. Therefore, it can show the quality of models rather than quality of estimates. When models have been built by different methods and have a different structure, other model quality indicators such as adjusted R^2 and Akaike information criterion (AIC) cannot be applied to all models with same assumptions. However, like AIC and unlike adjusted R^2 , the RMSE number itself is not meaningful because it depends on the total volume. Therefore, the RMSE for models at one test site cannot be directly compared with RMSE values for models at a different intersection test site. Similarly, the RMSE from one approach at the intersection cannot be compared with the RMSE values from another approach.

6. SUMMARY AND CONCLUSIONS

Current practice for automated calculation of turning movement proportions in shared lanes is to use downstream detectors in addition to stop bar detectors and traffic signal information. However, many cities do not have downstream detectors. In this paper, three different methods were proposed to calculate the proportion of turning vehicle movements in shared lanes at signalized intersections. These methods, wherever conditions are met, were easy to apply and did not need considerable investment. The methods were applied at three intersections in Reno, NV. The results from a case study indicated that these methods can be applied to produce accurate counts. GP was used for modeling and was found to generate more accurate models compared with conventional regression. Many DOT divisions and regional transportation agencies will likely benefit from this study in terms of traffic operations, safety, intermodal planning, traffic information, and performance analysis. These methods can be used for almost every kind of detectors besides the commonly used loop detectors.

REFERENCES

1. Tian J, Virkler M Sun C. Field testing for automated identification of turning movements at signalized intersections. *Transportation Research Record* 2004; **1867**: 210–216.
2. Sunkari S, Charara H, Urbanik T. Automated turning movement counts from shared lane configurations at signalized diamond interchanges. Transportation Research Board Annual Meeting 2000, Washington DC, 2000.
3. Mirchandani P, Nobe S Wu W. Online turning proportion estimation in real-time traffic-adaptive signal control. *Transportation Research Record* 2001; **1748**: 80–86.
4. Jiao P, Lu H, Yang L. Real-time estimation of turning movement proportions based on genetic algorithm. Proceedings of the 8th International IEEE Conference on Intelligent Transportation Systems, Vienna, Austria, 2005.
5. Lan C, Davis G. Real-time estimation of turning movement proportions from partial counts on urban networks. *Transportation Research Part C* 1999; 305–327.
6. Yi P, Shao C, Mao J. Development and preliminary testing of an automatic turning movements identification system. Final Report, Transportation Consortium, University of Akron. 2010.
7. Gentili M, Mirchandani P. Locating sensors on traffic networks: models, challenges and research opportunities. *Transportation Research Part C* 2012; 305–327.
8. Chen A, Chootinan P, Ryu S, Lee M Recker W. An intersection turning movement estimation procedure based on path flow estimator. *Journal of Advanced Transportation* 2012; **46**(2): 161–176.
9. FHWA. ITS data archiving: case study analyses of San Antonio TransGuide Data. Prepared by Texas Transportation Institutes. 1999.
10. ITE (Institute of Transportation Engineers). Using existing loops at signalized intersections for traffic counts. Institute of Transportation Engineers, 2007.
11. Middleton D, Parker R, Longmire R. Investigation of vehicle detector performance and ATMS interface. Texas Transportation Institute, Texas A&M University System, 2006. FHWA/TX-07/0-4750-2
12. Middleton D, Parker R. Vehicle detector evaluation. Texas Transportation Institute, Texas A&M University System. FHWA/TX-03/2119-1
13. Vanajakshi L, Rilett LR. Loop detector data diagnostics based on conservation-of-vehicles principle. *Transportation Research Record: Journal of the Transportation Research Board* No. 1870, TRB, National Research Council, Washington, D.C. 2004; 162–166.
14. Bender J, Nihan L. *Inductive Loop Detector Failure Identification: A State of the Art Review* Washington State Transportation Center: Olympia, 1988.
15. Jacobson LN, Nihan NL, Bender JD. Detecting erroneous loop detector data in a freeway traffic management system. *Transportation Research Record* 1287, TRB, National Research Council, Washington, D.C., 1990; 151–166.
16. Dudek CL, Messer CJ, Dutt AK. Study of detector reliability for a motorist information system on the gulf freeway. *Transportation Research Record* 495, TRB, National Research Council, Washington, D.C., 1974; 35–43.

17. Courage KG, Bauer CS, Ross DW. Operating parameters for main line sensors in freeway surveillance systems. Transportation Research Record 601, TRB, National Research Council, Washington, D.C., 1976; 19–28.
18. Pinnell C. Inductive loop detectors: theory and practice. FHWA, U.S. Department of Transportation, 1976.
19. Bikowitz EW, Ross SP. Evaluation and improvement of inductive loop traffic detectors. Transportation Research Record 1010, TRB, National Research Council, Washington, D.C., 1985; 76–80.
20. Chen L, May AD. Traffic detector errors and diagnostics. Transportation Research Record 1132, TRB, National Research Council, Washington, D.C., 1987; 82–93.
21. Cleghorn D, Hall FL, Garbuio D. Improved data screening techniques for freeway traffic management systems. Transportation Research Record 1320, TRB, National Research Council, Washington, D.C., 1991; 17–31
22. Koza JR. *Genetic Programming II: Automatic Discovery of Reusable Programs* MIT Press: Cambridge, MA, 1994.
23. Nihan L, Jacobson LN, Bender JD. Detector data validity. WA-RD 208.1. Washington State Transportation Center, Olympia, 1990.
24. Payne HJ, Thompson S. Malfunction detection and data repair for induction-loop sensors using I-880 Database. Transportation Research Record 1570, TRB, National Research Council, Washington, D.C., 1997; 191–201.
25. Sunkari S, Charara H, Songchitruksa P. A portable toolbox to monitor and evaluate signal operations. Transportation Research Board 2012 Annual Meeting. 2012.
26. Negnevitsky M. *Artificial Intelligence: A Guide to Intelligent Systems (2nd Edition)* Addison Wesley Publishers: England, 2004.
27. Gandomi AH, Alavi AH. *A new multi-gene genetic programming approach to non-linear system modeling. Part II: geotechnical and earthquake engineering problems, Neural Comput & Applic.* 2011. DOI: <http://dx.doi.org/10.1007/s00521-011-0735-y>
28. Searson DP, Leahy DE Willis MJ. GPTIPS: an open source genetic programming toolbox for multigene symbolic regression. In *Proceedings of the International MultiConference of Engineers and Computer Scientists 2010 (IMECS 2010)*: Hong Kong, 2010.